Final version published as: Shen, D. L., Liu, T.-W., Zandberg, W., Clark, T., Eskandari, R., Alteen, M. G., Tan, H. Y., Zhu, Y., Cecioni, S., & Vocadlo, D. (2017). Catalytic Promiscuity of O-GlcNAc Transferase Enables Unexpected Metabolic Engineering of Cytoplasmic Proteins with 2-Azido-2-deoxy-glucose. ACS Chemical Biology, 12(1), 206–213. https://doi.org/10.1021/acschembio.6b00876

Catalytic Promiscuity of *O*-GlcNAc Transferase Enables Unexpected Metabolic Engineering of Cytoplasmic Proteins with 2-Azido-2-deoxy-glucose

David L. Shen,[†,‡] Ta-Wei Liu,[†,‡] Wesley Zandberg,[†] Tom Clark,[†] Razieh Eskandari,[†] Matthew G. Alteen,[†] Hong Yee Tan,[†] Yanping Zhu,[†,‡] Samy Cecioni,[†] and David Vocadlo*[,†,‡]

[†]Department of Chemistry, Simon Fraser University, Burnaby, British Columbia V5A 1S6, Canada

[‡]Department of Molecular Biology and Biochemistry, Simon Fraser University, Burnaby, British Columbia V5A 1S6, Canada

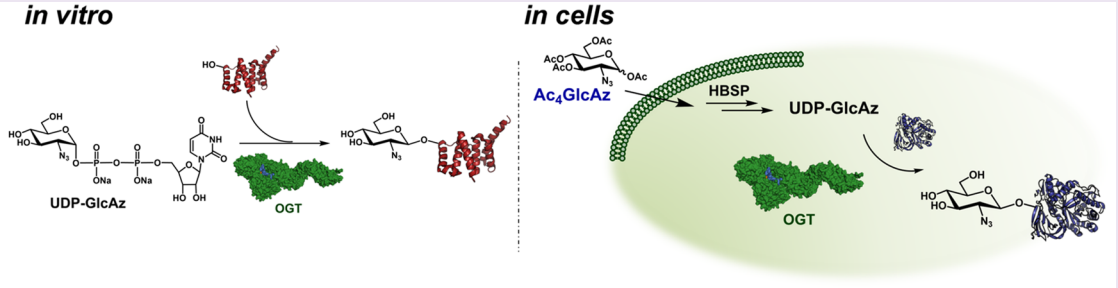

ABSTRACT: *O*-GlcNAc transferase (OGT) catalyzes the installation of *N*-acetylglucosamine (GlcNAc) *O*-linked to nucleocytoplasmic proteins (*O*-GlcNAc) within multicellular eukaryotes. OGT shows surprising tolerance for structural changes in the sugar component of its nucleotide sugar donor substrate, uridine diphosphate *N*-acetylglucosamine (UDP-GlcNAc). Here, we find that OGT uses UDP-glucose to install *O*-linked glucose (*O*-Glc) onto proteins only 25-fold less efficiently than *O*-GlcNAc. Spurred by this observation, we show that OGT transfers 2-azido-2-deoxy-D-glucose (GlcAz) *in vitro* from UDP-GlcAz to proteins. Further, feeding cells with per-*O*-acetyl GlcAz (AcGlcAz), in combination with inhibition or inducible knockout of OGT, shows OGT-dependent modification of nuclear and cytoplasmic proteins with *O*-GlcAz as detected using microscopy, immunoblot, and proteomics. We find that *O*-GlcAz is reversible within cells, and an unidentified cellular enzyme exists to cleave *O*-Glc that can also process *O*-GlcAz. We anticipate that AcGlcAz will prove to be a useful tool to study the *O*-GlcNAc modification. We also speculate that, given the high concentration of UDP-Glc within certain mammalian tissues, *O*-Glc may exist within mammals and serve as a physiologically relevant modification.

The modification of serine and threonine residues of nucleocytoplasmic proteins with β-*O*-linked *N*-acetylglucosamine (*O*-GlcNAc) is widespread and conserved among metazoans. *O*-GlcNAc has been implicated in the diverse cellular processes ranging from transcription[1] to stress response.[2] Imbalances in *O*-GlcNAc levels have accordingly been implicated in various diseases including, for example, Alzheimer disease[3] and cancer.[4] Two carbohydrate-processing enzymes act to regulate cellular *O*-GlcNAc levels. The enzyme catalyzing the installation of *O*-GlcNAc using uridine diphosphate-α-*N*-acetyl-D-glucosamine (UDP-GlcNAc) as the glycosyl donor is the glycosyltransferase uridine diphosphate-*N*-acetyl-D-glucosamine: polypeptidyl transferase (OGT).[5] The enzyme responsible for catalyzing the removal of *O*-GlcNAc is the glycoside hydrolase known as *O*-GlcNAcase (OGA).[5] Given the important and wide ranging roles played by *O*-GlcNAc, there is considerable interest in understanding the substrate specificities[5−8] of these enzymes as well as the development of chemical probes that can be used to interrogate the function of *O*-GlcNAc.[7,9−13]

Supporting a critical conserved role in cell function, OGT is present within all eukaryotes and in all mammalian tissues as two isoforms, which arise from alternative splicing of the *OGT* gene.[5] Recently, the structure of a major fragment of human OGT (hOGT) was reported, comprising the C-terminal catalytic domain and the first 4.5 tetratricopeptide repeats (TPRs) of the N-terminal TPR-containing region.[14,15] The structure of this hOGT construct in a ternary complex[15] with uridine diphosphate-*N*-acetyl-D-5-thioglucosamine (UDP-5SGlcNAc),[16] an incompetent substrate analogue of UDP-GlcNAc, and a peptide substrate reveals details of active site enzyme−substrate interactions. This model indicates that the nitrogen of the acetamide group of UDP-5SGlcNAc hydrogen bonds with one of the β-phosphate oxygens of the diphosphate moiety and its carbonyl group hydrogen bonds with His498. Notably, site-directed mutagenesis of His498 impairs OGT

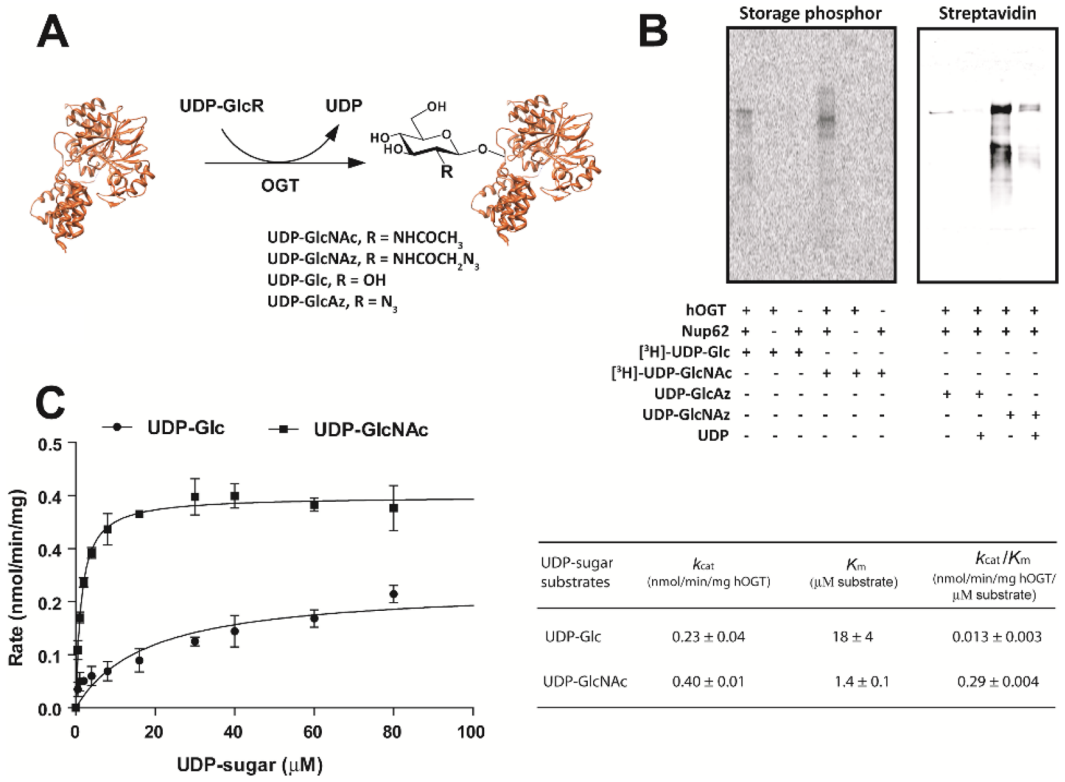

UDP-sugar substrates	k_{cat} (nmol/min/mg hOGT)	K_m (μM substrate)	k_{cat}/K_m (nmol/min/mg hOGT/ μM substrate)
UDP-Glc	0.23 ± 0.04	18 ± 4	0.013 ± 0.003
UDP-GlcNAc	0.40 ± 0.01	1.4 ± 0.1	0.29 ± 0.004

Figure 1. UDP-Glc and UDP-GlcAz, competent nucleotide sugar donor substrates for hOGT *in vitro*. (A) Schematic showing the hOGT catalyzed glycosyl transfer using different nucleotide sugar donor substrates. (B) Blotting of Nup62 incubated with hOGT and radiolabeled UDP-Glc and UDP-GlcNAc (4 μM, left panel) or UDP-GlcAz and UDP-GlcNAz (100 μM, right panel) as sugar donor substrates. hOGT catalyzed transfer of [^{3}H]-UDP-GlcNAc and UDP-GlcNAz at the same concentrations used for UDP-Glc and UDP-GlcAz, respectively. CuAAC labeling of GlcAz and GlcNAz labeled proteins was performed using alkyne-diazo-biotin and visualization using streptavidin IRdye. (C) Kinetic analysis of the hOGT catalyzed transfer of UDP-GlcNAc (closed circles) and UDP-Glc (closed squares) at various concentrations using a fixed Nup62 concentration (10 μM). The resulting kinetic parameters are summarized in the table. The data are displayed as an average of quadruplicate determinations with associated standard deviations shown as error bars.

activity,[17] consistent with this model and supporting a critical role for the acetamido group in catalysis.[14]

Here, we describe our surprising observation that OGT could transfer glucose from uridine diphosphate-D-glucopyranose (UDP-glucose, UDP-Glc) to the well-known OGT substrate nucleoporin 62 (Nup62).[18,19] Stimulated by this observation, we went on to show that uridine diphospho-2-azido-2-deoxy-α-D-glucopyranose (UDP-GlcAz) serves as a substrate of hOGT *in vitro*. We further demonstrated that feeding cells with 1,3,4,6-*tetra*-*O*-acetyl-2-azido-2-deoxy-D-glucopyranose (AcGlcAz) resulted in labeling of cellular proteins, including Nup62, with *O*-linked 2-azido-2-deoxy-β-D-glucose (*O*-GlcAz). Given the distribution of *O*-GlcAz-labeled proteins within cells, as assessed by microscopy, in conjunction with the identity of proteins metabolically labeled with GlcAz established using mass spectrometry (MS) proteomics, we conclude that OGT shows surprising substrate promiscuity and that AcGlcAz can be assimilated within cells to label nuclear and cytoplasmic proteins in place of *O*-GlcNAc. We anticipate that this metabolic labeling substrate may prove useful to study the roles of *O*-GlcNAc and aid in identification of specific subsets of *O*-GlcNAc glycosylated proteins. Finally, these data suggest OGT is more promiscuous than previously recognized and may catalyze modification of proteins with naturally occurring sugars other than *O*-GlcNAc, such as *O*-Glc.

RESULTS AND DISCUSSION

UDP-Glc and UDP-GlcAz Are Substrates of OGT. During routine *in vitro* assays to monitor hOGT transferase activity using UDP-[^{3}H]GlcNAc,[6,17] we unexpectedly observed glucosyltransferase activity when using UDP-[^{3}H]Glc as a negative control donor substrate with Nup62 as the acceptor protein (Figure 1A and B). To test whether the UDP-[^{3}H]Glc might be contaminated with UDP-[^{3}H]GlcNAc we performed immunoblot using anti-*O*-GlcNAc antibody and found there was no detectable immunoreactivity against [^{3}H]Glc-modified Nup62 (Supporting Figure 2). We also performed parallel kinetic studies using UDP-[^{3}H]Glc and UDP-[^{3}H]GlcNAc (Figure 1C). For UDP-Glc, we find k_{cat} and K_m values that are distinct from the values obtained using UDP-GlcNAc as the donor substrate (Figure 1C). These data indicate there was no contamination of the commercial supply of UDP-Glc. Notably, we observe that the second order rate constant (k_{cat}/K_m) for UDP-Glc as a donor substrate was only 25-fold lower than that measured when using UDP-GlcNAc. The major difference in k_{cat}/K_m values stemmed from the 13-fold higher K_m value for UDP-Glc as compared to UDP-GlcNAc, which is consistent with the 2-acetamido group forming binding interactions with the hOGT active site.

We therefore speculated that hOGT might tolerate replacement of the 2-acetamido substituent and considered whether a group incapable of hydrogen bonding to the enzyme would be tolerated. We therefore synthesized uridine

diphosphate-2-azido-2-deoxy-D-glucopyranose (UDP-GlcAz, Figure 1A, Supporting Figure 1, and Supporting Methods) and uridine diphosphate-2-azidoacetyl-2-deoxy-D-glucopyranose (UDP-GlcNAz, Figure 1A).[9] We used these compounds as substrates for hOGT using chemoselective copper-catalyzed azide–alkyne cycloaddition (CuAAC)[20,21] to detect transfer of the sugar moiety onto protein substrates. Both GlcAz and GlcNAz were transferred onto Nup62 with, as expected given the second order rate constants for UDP-GlcNAc versus UDP-Glc (Figure 1C), a strong preference for UDP-GlcNAz over UDP-GlcAz (Figure 1B, right panel). Previous reports indicate that the different reactivities[20,21] of the primary and secondary azide moieties of these donor sugars should not significantly affect the coupling reaction, suggesting that the click chemistry used here should not contribute significantly to errors in these observations.

We were curious whether human OGA (hOGA), a β-glucosidase, or mammalian cell lysates might be able to remove either *O*-Glc or *O*-GlcAz from proteins. We thus incubated recombinant Nup62, modified using either UDP-[^{3}H]GlcNAc or UDP-[^{3}H]Glc, with hOGA, sweet almond β-glucosidase, and COS-7 crude cell lysates (Figure 2A). We find as expected that

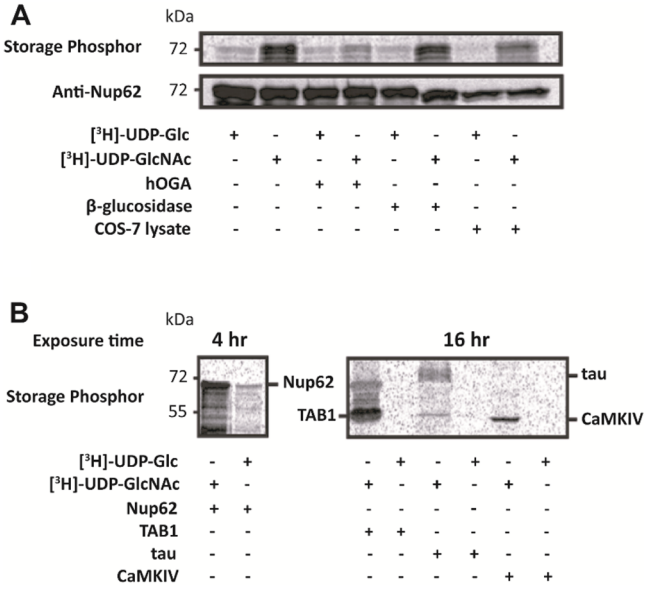

Figure 2. Characterization of the OGT catalyzed formation of *O*-Glc and *O*-GlcNAz and their processing by hOGA and β-glucosidases *in vitro*. (A) hOGT radiolabeled *O*-Glc and *O*-GlcNAc modified Nup62 were subjected to digestion by hOGA, sweet almond β-glucosidase, and COS-7 cell lysates. (B) Assay of hOGT-catalyzed formation of *O*-Glc using Nup62, TAB1, tau, and CaMKIV.

hOGA could remove [^{3}H]GlcNAc but left [^{3}H]Glc attached to the Nup62. The β-glucosidase processed neither substrate; however, [^{3}H]Glc was removed from Nup62 *in vitro* at neutral pH in the presence of COS-7 cell lysates, suggesting there may be a cellular β-glucosidase that might prevent adventitious formation of *O*-Glc within cells. We next evaluated several proteins known to be *O*-GlcNAc modified including TAK1-binding protein 1 (TAB1),[22] the full length microtubule associated protein tau (isoform 2N4R),[23] and calcium/calmodulin-dependent protein kinase type IV (CaMKIV)[24] as substrates for the hOGT-catalyzed formation of *O*-Glc/*O*-GlcNAc using UDP-[^{3}H]Glc/UDP-[^{3}H]GlcNAc as sugar donors (Figure 2B). Curiously, among these four protein substrates, which were modified using UDP-[^{3}H]GlcNAc, only Nup62 was modified by UDP-[^{3}H]Glc. We also evaluated the ability of OGT to use UDP-GlcNAc, UDP-Glc, and UDP-GlcAz as donor substrates for the OGT catalyzed modification of the known OGT peptide substrate CKII.[14] Qualitatively, OGT could modify CKII with UDP-GlcNAc and UDP-Glc, though as expected, UDP-Glc is used less efficiently than UDP-GlcNAc (Supporting Figure 3). We find that using these conditions, OGT transfer using UDP-GlcAz as a donor substrate for the CKII peptide was not detected, which may stem from it being a poor substrate *in vitro* with this acceptor peptide substrate. These observations suggest that *O*-Glc modification catalyzed by OGT is relatively inefficient and may (i) occur with some preference for certain protein substrates, (ii) require other components only found *in vivo* for efficient transfer, or (iii) occur at a slow rate such that it can only be observed using excellent protein acceptor substrates.

Substrate Engineering Using GlcAz. Recent efforts have enabled metabolic labeling of *O*-GlcNAc modified proteins in cell culture.[7,9−13,25] These sugar analogues make use of acetyled precursor sugars that are deacylated within the cell by endogenous esterases. Given the unusual observation that UDP-GlcAz can serve as a substrate for hOGT, we set out to establish whether UDP-GlcAz was formed in COS-7 cells cultured with AcGlcAz (Supporting Figure 4A). Using capillary electrophoresis (CE) to detect nucleotide sugars,[16] we found that COS-7 cells treated with 100 μM AcGlcAz produced two nucleotide azido-sugars which could be detected after CuAAC labeling with Fluor488-alkyne. One is UDP-GlcAz based on its co-migration with a synthetic standard, and the other is thought to be UDP-GalAz, converted from UDP-GlcAz by a UDP-GlcNAc/Glc-epimerase to yield the expected relative levels predicted to be produced by UDP-GlcNAc/Glc-epimerase.[26] Treating cells with GlcAz or DMSO vehicle control resulted in little to no labeling (Supporting Figure 5B), whereas AcGlcAz led to dose-dependent labeling of cellular proteins (Figure 3A and Supporting Figure 5C). We observed time-dependent increases in protein labeling up to 16 h after AcGlcAz treatment (Supporting Figure 5D). These time-dependent data suggest preferential labeling of certain proteins that can be seen at early time points. We find *O*-GlcAz is gradually lost from proteins after changing the media (Supporting Figure 5E), presumably either through enzymatic processing as suggested by our *in vitro* studies (Figure 2A) or during their proteolytic degradation. Notably, we observed a similar protein pattern in DMSO-treated and 100 μM AcGlcAz-treated COS-7 lysates, but different patterns were seen in lysates from cells treated with 250 μM AcGlcAz (Supporting Figure 5A), which is consistent with concentrations of AcGlcAz $\geq$ 250 μM having marked effects on cell morphology at 16 h.

To test if AcGlcAz influences *O*-GlcNAc levels, we performed immunoblot analyses using anti-OGT and anti-*O*-GlcNAc antibodies and found a decrease in both OGT and *O*-GlcNAc levels upon AcGlcAz treatment at 16 h (Figure 3A). Given the apparent decrease in *O*-GlcNAc levels, and because OGT levels are known to drop upon increased cellular *O*-GlcNAcylation,[16] we speculated that accumulated *O*-GlcAz on proteins may compete with *O*-GlcNAc. Alternatively, formation of UDP-GlcAz may compete with UDP-GlcNAc levels, leading to decreased UDP-GlcNAc levels upon AcGlcAz treatment and consequent decreased *O*-GlcNAc levels that are independent of *O*-GlcAz levels. Our CE analysis of UDP-GlcNAc, UDP-GalNAc, UDP-Glc, and UDP-Gal levels within COS-7 cells

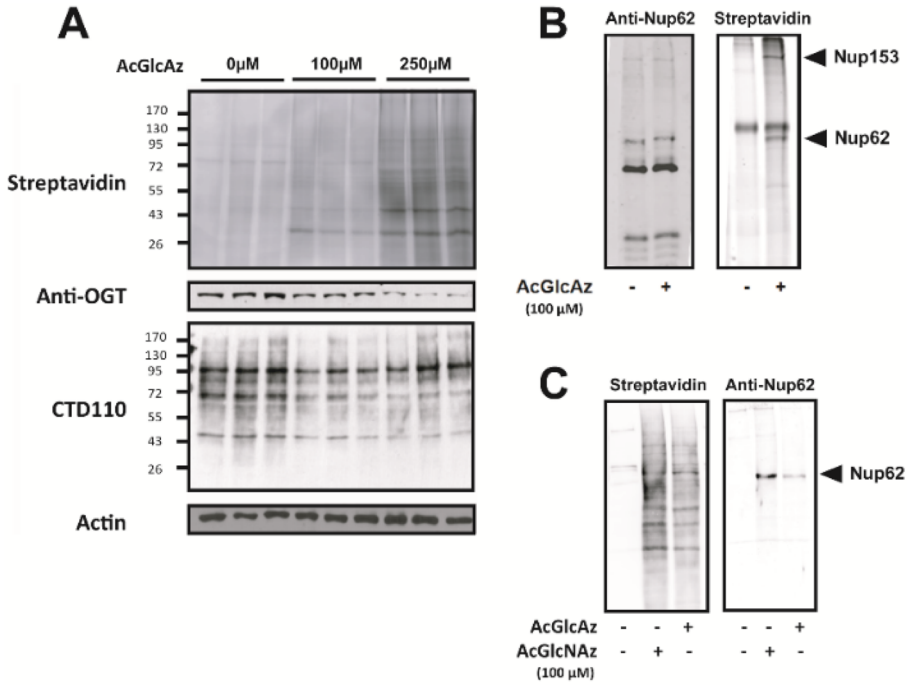

Figure 3. Characterization *O*-GlcAz labeling in whole cell lysates and on Nup62. (A) Dose-dependent effects of 16 h treatment with AcGlcAz (100 or 250 μM) on COS-7 cell labeling using CuAAC labeling with 5-TAMRA-alkyne. Effect of AcGlcAz on OGT and *O*-GlcNAc levels as assessed by immunoblot. (B) Immunoprecipitation of Nup62 and Nup153 from COS-7 cells using mAb414 and their detection using mAb414 and CuAAC conjugation to a biotin probe followed by streptavidin blotting. (C) CuAAC conjugation of lysates to a biotin probe followed by streptavidin pulldown and probing using mAb414.

(Supporting Figure 4B) show that AcGlcAz has no significant effect on the levels of these UDP-nucleotide sugars.

We next evaluated whether GlcAz is found on known targets of OGT. We therefore immunoprecipitated the well-known OGT target protein Nup62 from COS-7 cell lysates treated with 100 μM AcGlcAz (Figure 3B). We find monoclonal antibody mAb414, which targets nucleoporins containing FG repeats including Nup62 and Nup153, immunoprecipitated nucleoporins that could be labeled by CuAAC using a cleavable alkyne-diazo-biotin probe and detected by streptavidin blotting. The reverse experiment using CuAAC to first install the alkyne-diazo-biotin and precipitate labeled proteins using streptavidin yielded a pool of proteins in which we could detect Nup62 by immunoblot using mAb414 (Figure 3C). These data provide clear support for *O*-GlcAz labeling of nucleocytoplasmic proteins upon metabolic feeding with AcGlcAz.

OGT Inhibition and Knockdown Reduce *O*-GlcAz. To estimate the extent of OGT-dependent GlcAz incorporation into nuclear and cytosolic proteins, we used both chemical and genetic methods to reduce cellular OGT activity (Figure 3). We used 1,3,4,6-*tetra*-*O*-acetyl-5-thio-α-D-glucopyranose (Ac5SGlcNAc) as a cell active OGT inhibitor to decrease OGT activity.[16] Using mouse embryonic fibroblasts (MEFs)[2] that regulate Cre-recombinase in a tamoxifen-inducible manner, we induced site-specific excision of the *OGT* gene and downstream loss of OGT protein and *O*-GlcNAc. Treating MEF cells with tamoxifen or Ac5SGlcNAc both resulted in a robust decrease in *O*-GlcAz protein modification (Figure 4B). Deletion of OGT from MEF cells was confirmed by decreases in both OGT and *O*-GlcNAc levels (Figure 3). Next, we investigated whether GlcAz is incorporated into *N*-linked glycans at significant levels by using PNGase *F* digestion to remove glycoprotein *N*-glycosylation in lysates from AcGlcAz-treated COS-7 cells. We observed no reduction in the level of GlcAz-dependent protein-linked azide groups. We also assessed the effects of AcGlcAz on protein *N*-glycosylation levels and found there was a decrease in the level of ConA reactivity in the AcGlcAz treated COS-7 cell lysate, but we observed no change in WGA reactivity (Supporting Figure 6). Similar to the effect of 2-deoxy-D-glucose on cells,[27] we speculate that AcGlcAz could reduce the amount of dolicol-linked Glc and GlcNAc donors and thereby impede early steps of *N*-glycan biosynthesis. Collectively, these data suggest that GlcAz is not significantly incorporated into *N*-glycans and does not result in major perturbations in nucleotide sugar levels.

To evaluate the cellular locations at which GlcAz is incorporated we fixed COS7 cells and then conjugated 5-TAMRA-alkyne to azide moieties. We again noted that 250 μM AcGlcAz led to changes in cell morphology that were consistent with the observed perturbations in the cellular protein composition (Supporting Figure 5A). At 100 μM AcGlcAz, however, we observed no obvious morphological changes and noted prominent protein labeling within the nucleocytoplasmic space (Supporting Figure 7). Using MEF cells, we observed similar effects at 100 μM AcGlcAz, with the majority of fluorescence being localized to the nucleus and the nuclear envelope (Figure 4A), which is consistent with nuclear pore proteins being major targets of OGT.[19,28] Interestingly, the *O*-GlcAz signal forms punctuate structures having sizes ranging from 0.8 to 1.2 μm that appear to be qualitatively coincident with the Hoechst staining. AcGlcNAz labeling (100 μM) observed using quantitative wide-field fluorescence microscopy revealed a similar level of labeling to when using GlcAz (GlcAz, 100 $\pm$ 6 RFU/cell; GlcNAz, 95 $\pm$ 7 in RFU/cell). The metabolic OGT inhibitor Ac5SGlcNAc caused a reduction in *O*-GlcAz labeling (30 $\pm$ 2 RFU/cell) similar to that seen when

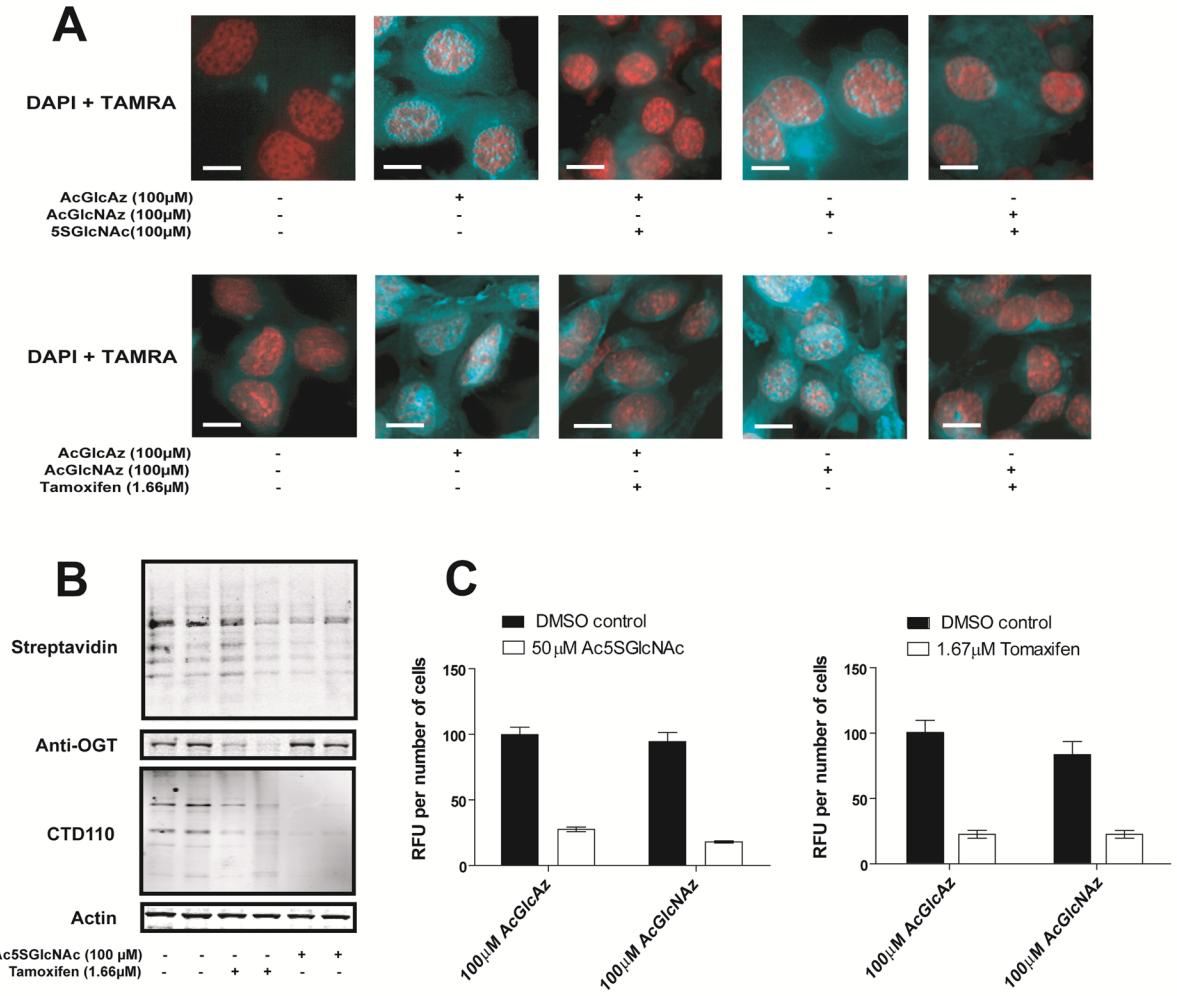

Figure 4. Quantitative widefield fluorescence imaging of MEF cells treated with AcGlcAz and AcGlcNAz. Red indicates DAPI staining, and teal indicates GlcAz-dependent fluorescence arising from CuAAC conjugation with 5-TAMRA-alkyne. (A) Effect of treatment with 5SGlcNAc (50 μM) or excision of the OGT gene by tamoxifen (1.66 μM) on TAMRA fluorescence. The white bar at the left corner represents 10 μm. (B) Immunoblot analysis of the effects in MEF cells of OGT gene excision induced by tamoxifen (1.66 μM) or inhibition of OGT inhibition by Ac5SGlcNAc (100 μM). (C) Quantitative analysis is carried out for each condition by dividing the TAMRA fluorescence by the number of cells in the field. All measurements were made in quadruplicate.

using this inhibitor with GlcNAz (21 ± 1 RFU/cell). Notably, loss of O-GlcAz labeling was most pronounced within the nucleus, leading to disappearance of the punctuate *O*-GlcAz-labeled features. Tamoxifen-induced knockout of OGT in MEF cells also decreased *O*-GlcAz and *O*-GlcNAz labeling (GlcAz, 100 ± 9 to 23 ± 3 RFU/cell; GlcNAz, 83 ± 10 to 23 ± 3 RFU/cell) resembling that seen when using Ac5SGlcNAc. These data provide strong support for GlcAz being incorporated predominantly as O-GlcAz onto nuclear and cytoplasmic proteins.

Proteomics of *O*-GlcAz Modified Proteins. To identify O-GlcAz labeled proteins, we next adopted established methods to chemoselectively enrich azide-tagged proteins,[10] here using an alkyne-diazo-biotin cleavable probe and bound resulting tagged proteins to streptavidin resin (Supporting Figure 8). In parallel, we processed cells which had not been treated with AcGlcAz. After releasing the proteins from the probe with sodium dithionite and subjecting them to SDS-PAGE, we proteolytically digested the samples and subjected the resulting peptides to nanoLC-MS/MS analysis. Using this approach, we identified 64 proteins in the experimental sample using a 5% false positive threshold and only keratins and two others in the control sample (Supporting Tables 1 and 2). All of the identified proteins were nuclear or cytoplasmic, and all but two are known *O*-GlcNAcylated proteins. Among these proteins are two involved in carbohydrate metabolism, fructose-bisphosphate aldolase A[29] and pyruvate kinase PKM (PKM2).[30] We also observed several cytoskeletal proteins including vimentin[31] and mitochondrial proteins such as voltage-dependent anion-selective channel protein 3 (VDAC3)[32] (Supporting Figure 9). Notably, none of the identified proteins were exclusively secretory proteins, which supports that *O*-GlcAz predominantly occurs on nuclear and cytoplasmic proteins.

Conclusions. Here, we found, surprisingly, that OGT can use UDP-Glc as a donor substrate with a good acceptor protein substrate such as Nup62.[6,18] These data suggest that within cells, the adventitious installation of glucose to form *O*-Glc modified proteins may occur at low levels in a manner analogous to the infrequent translational misincorporation seen during protein synthesis.[33] The extent of OGT-catalyzed formation of *O*-Glc, as compared to *O*-GlcNAc, would be

governed by the ratio of the second order rate constants (k_{cat}/K_m) for each of the donor sugar substrates multiplied by the ratio of the nucleotide donor sugar concentrations. Accordingly, with comparable levels of UDP-Glc and UDP-GlcNAc within cells (Supporting Figure 4B), we would expect that one out of every 25 *O*-GlcNAc residues on Nup62 would be replaced with *O*-Glc. Notably, UDP-Glc is an abundant sugar nucleotide that is biosynthesized from glucose and used in the synthesis of glycogen, which acts as an energy reserve in specific tissues. Levels of UDP-Glc therefore reflect glucose availability,[34] and levels can at times reach the hundred micromolar concentration range within certain tissues.[35] Accordingly, it seems possible that *O*-Glc is a modification that cells may need to cope with through the presence of a β-glucosidase having activity against such a glycoconjugate. Consistent with a requirement for the 2-acetamido group of the substrate for catalysis by hOGA,[36] we find that OGA cannot remove *O*-Glc. However, COS-7 lysates catalyze the removal of *O*-Glc from modified Nup62, suggesting a neutral β-glucosidase may be present within cells. Accordingly, we speculate that further research may reveal the presence of *O*-Glc within certain tissues having high UDP-Glc to UDP-GlcNAc ratios.

Motivated by this *in vitro* promiscuity shown by OGT, we showed that UDP-GlcAz was also a substrate *in vitro* for the hOGT catalyzed modification of Nup62. We note that 2AzGlc is unlikely to enter central metabolism since neither 2-deoxy- nor 2-deoxy-2-fluoro-glucose are metabolized in this fashion.[37] Instead, we found that metabolic feeding of cells with AcGlcAz resulted in the formation of *O*-GlcAz conjugates within cells that are localized primarily to nuclear and cytoplasmic proteins. The use of both chemical and genetic methods to reduce OGT activity supports GlcAz being incorporated within cells as *O*-GlcAz conjugates. Nevertheless, it is possible that GlcAz can be assimilated into glucose-containing glycoconjugates that were not examined. Curiously, we observed OGT-dependent formation of *O*-GlcAz conjugates in what appear to be heterochromatic foci, consistent with proposed roles for OGT in gene repression.[38−40] We also noted the presence of β-glucosidase activity within COS-7 lysates that is capable of processing *O*-GlcAz from proteins, which is consistent with the relatively rapid time-dependent decrease in *O*-GlcAz levels observed upon removing this metabolic precursor from the media. Notably, AcGlcAz treatments at 250 μM and above show obvious cytotoxicity, which bears some similarity to observations showing that 2-deoxy-D-glucopyranose (2-DG) gives rise to cytotoxicity through multiple mechanisms.[41,42] Worth noting in this regard is that 2-DG has been shown to modulate *O*-GlcNAc levels[43] through a mechanism that is not well established, perhaps 2-DG is also incorporated onto proteins at some level.[27]

It is interesting to speculate on the potential physiological implications of these findings. UDP-Glc levels rise profoundly upon increased glucose influx.[34,44] In humans, the hepatic assimilation rate of glucose into UDP-Glc increases from 0.2 mg/kg/min during fasting to 1.3−1.6 mg/kg/min on oral feeding, and this represents approximately 20% of the consumed carbohydrate load.[45] Under such conditions, increased OGT catalyzed modification of proteins with *O*-Glc might occur, and such modification may play physiological roles within cellular nutrient sensing pathways. This hypothesis, however, remains speculative since *O*-Glc has not been detected within cells and *O*-GlcAz formation and processing may not reflect the potential cellular processing of *O*-Glc. Accordingly, a method to detect the *O*-Glc modification within cells could be of interest to address whether *O*-Glc is present and, if so, whether it might occur within specific tissues at levels consistent with function or at levels consistent with what might be considered normal metabolic misincorporation. Finally, we anticipate that AcGlcAz will serve, in a manner that is complementary to other metabolic labeling reagents for *O*-GlcNAc, as a useful chemical probe for cellular studies to identify certain sets of protein that are particularly good substrates for OGT.

METHODS

hOGT Assay. Nonradioactive hOGT assays were carried out using 100 μM UDP-GlcAz or UDP-GlcNAz, 10 μM recombinant Nup62, and 1 μM hOGT at 37 °C for 2 h. The reactions were terminated by the addition of 0.1 mM UDP.[46] Click chemistry to couple the GlcAz- and GlcNAz-labeled Nup62 using alkyne-diazo-biotin was performed and detected using streptavidin IRdye. Radioactive hOGT assays were performed, as described previously,[6] using recombinant Nup62 as the protein acceptor, and [^{3}H]-UDP-GlcNAc (American Radiolabeled Chemicals) or [^{3}H]-UDP-Glc (American Radiolabeled Chemicals) as the sugar donor. The specific activities of [^{3}H]-UDP-GlcNAc and [^{3}H]-UDP-Glc were standardized to 4.3 Ci mmol^{-1}. All assays were done in at least triplicate. The counts in disintegrations per minute (dpm) from scintillation counting were converted into rates (μmol of GlcNAc min^{-1} mg^{-1} of hOGT) taking into account the length of time for the assay and the enzyme concentration. The background rate in the absence of enzyme was subtracted, and the resulting initial rates were plotted against the substrate concentration using GRAFIT[47] to establish the apparent k_{cat} and K_m values for each substrate, which for simplicity are referred to below as k_{cat} and K_m values. Radiolabeling of recombinant Nup62, TAB1, CaMKIV, and tau (Isoform 2N4R) were carried out using 100 μM of [^{3}H]-UDP-GlcNAc or [^{3}H]-UDP-Glc with 4.3 Ci mmol^{-1} specific activity as the sugar donor, 10 μM protein substrates, and 0.5 μM hOGT at 37 °C for 2 h. The reactions were quenched with 0.1 mM UDP. Laemmli buffer was added to each of the samples and subjected to SDS-PAGE and transferred onto a nitrocellulose membrane. The membrane was air-dried before exposure to a tritium phosphor imaging screen (GE Healthcare). Four and 16 h exposures were scanned by a Typhoon Imager 8600 (Amersham) using the storage phosphor mode. The best contrast and brightness of the figures were achieved using ImageQuant 5.2 (Molecular Dynamics).

Streptavidin Resin Capture. COS-7 cells in 25 cm^2 plates were allowed to grow to 80% confluency before being treated with either 100 μM AcGlcAz or AcGlcNAz for 16 h. Cell pellets were collected and stored at 80 °C until required. Alkyne-diazo-biotin (0.5 mM) was incubated with streptavidin agarose beads (ThermoFisher) for 2 h at 4 °C in PBS-T with 1% BSA. The resin was then washed with 6 × 1 mL of PBS. Cell extracts were prepared by resuspending the cell pellet in a lysis buffer (100 mM sodium phosphate, pH 7.5, 1% Nonidet P-40, 150 mM NaCl, and protease and phosphatase inhibitor cocktail (Pierce)) and lysed by sonication. In order to remove the glycolipid contamination, protein was precipitated from the total lysate by chloroform/methanol precipitation. Precipitated proteins were pelleted by centrifugation at 14 000 rpm for 5−10 min at RT and washed twice with four volumes of methanol. The supernatant was removed without disturbing the pellet, and the pellet was air-dried. The protein pellet was dissolved in 1% SDS with heating and vortexing and was then subjected to click chemistry by mixing with the alkyne-diazo-biotin−streptavidin conjugated resin for 1 h at RT. The resin was washed with 3 × 1 mL 1% SDS in PBS and 3 × 1 mL PBS and then eluted using 100 mM sodium dithionite. The eluent was boiled and vortexed in Laemmli sample buffer. Western blot analysis was carried out on the samples to detect Nup62 using mAb414 antibody as described above.

hOGA, β-Glucosidase, and COS-7 Cell Lysate Digestions. Radiolabeling of recombinant Nup62 with [^{3}H]-UDP-GlcNAc or

[^{3}H]-UDP-Glc was carried out as described above. Recombinant hOGA was dialyzed into PBS and concentrated to approximately 10 μM using a centrifugal concentrating device with a 30 kDa MW cutoff (Amicon). β-Glucosidase from almond extract was purchased from Sigma. The COS-7 cell lysate was prepared by cell harvesting as described above. The cell pellet was resuspended in PBS with 0.1% nonyl phenoxylpolyethoxylethanol (NP-40) substitute (Fluka) and protease inhibitor cocktail (Roche). The lysate was then sonicated on ice at 20% intensity for 10 s (Fisher Scientific, Model 500) and centrifuged (13 000 rpm, 10 min, 4 °C) to remove insoluble debris. The final concentration of enzymes and lysate used to digest 8 μM [^{3}H]-UDP-GlcNAc or [^{3}H]-UDP-Glc labeled Nup62 were 2 μM hOGA, 10 unit mL^{-1} β-glucosidase, and 0.2 mg mL^{-1} cell lysate. PBS added to Nup62 samples was used as a control. After 2 h of incubation at 37 °C, the reactions were terminated by the addition of Laemmli sample buffer and analyzed by Typhoon Imager as described above.

Microscopy. COS-7 cells were plated into the central 60 wells of glass-bottom 96-well plates (Corning 4580) before the addition of AcGlcAz at 100 or 250 μM and incubation for 16 h. MEF cells were plated into the central 60 wells of tissue culture treated cyclic olefin-bottom 96-well plates (Corning 4680) and allowed to reach 60% confluence before 1.66 μM tamoxifen citrate (Bioshop) or 50 μM Ac5SGlcNAc was added to the cultures and incubated together for 24 h prior to the addition of either 100 μM AcGlcAz or AcGlcNAz and incubation for a further 16 h. Cells were washed with 4 °C PBS and fixed in a solution of 4% paraformaldehyde in PBS at 37 °C for 10 min. The cells were then permeabilized using 0.3% Trixon X-100. Click chemistry was carried using 5-carboxytetramethylrhodamine-alkyne (5-TAMRA-Alkyne; Click Chemistry Tools) for 1 h as described in the Supporting Methods. The cells were incubated with Hoechst nucleus stain for 20 min followed by washing with PBS. The cells were imaged using an ImageXpress Micro XLS Widefield High-Content Analysis System (Molecular Device) equipped with an APO 40× Nikon lens. TRITC (557/576 nm, Ex/Em) and Hoechst (352/461 nm, Ex/Em) channels were sequentially collected at 40× magnification. Four fields of images were acquired at predefined regions of each well of the microplate from each of three wells per treatment condition. Data were analyzed using MetaExpress image analysis software (Molecular Devices) by determining the total intensity obtained from the RFP channel and dividing by the number of cells in an individual field (containing at least 50 cells), chosen randomly from two of the fields obtained per well, to yield a mean value for RFU per cell (RFU/cell).

Additional Methods. Please see the Supporting Information for detailed methods describing synthetic procedures, recombinant protein expression and purification, cell culture, copper-catalyzed azide−alkyne cycloaddition reactions, SDS-PAGE and immunoblot analysis, immunoprecipitation of Nup62, hOGT assay using CKII peptide as sugar acceptor PNGase F N-glycosylation digestion, analysis of sugar nucleotides in cells by capillary electrophoresis, and mass spectrometry proteomics.

■ ASSOCIATED CONTENT

Supporting Information

The Supporting Information is available free of charge on the ACS Publications website at DOI: 10.1021/acschembio.6b00876.

Supporting Figures 1−9, Tables 1 and 2, and Methods (PDF)

■ AUTHOR INFORMATION

Corresponding Author

*E-mail: dvocadlo@sfu.ca.

ORCID

David Vocadlo: 0000-0001-6897-5558

Notes

The authors declare no competing financial interest.

■ ACKNOWLEDGMENTS

Financial support through a Discovery Grant for Natural Sciences and Engineering Research (D.V., NSERC, RGPIN/-2015-05426) and the Canadian Institutes of Health Research (D.V., D.L.S., CIHR, MOP-102756) is gratefully acknowledged. D.V. acknowledges the kind support of the Canada Research Chairs program for a Tier I Canada Research Chair in Chemical Glycobiology and NSERC for support as an E.W.R. Steacie Memorial Fellow. S.C. thanks the CIHR for a postdoctoral fellowship.

■ REFERENCES

(1) Zhang, Z., Costa, F. C., Tan, E. P., Bushue, N., DiTacchio, L., Costello, C. E., McComb, M. E., Whelan, S. A., Peterson, K. R., and Slawson, C. (2016) O-Linked N-Acetylglucosamine (O-GlcNAc) Transferase and O-GlcNAcase Interact with Mi2beta Protein at the Agamma-Globin Promoter. *J. Biol. Chem. 291*, 15628−15640.

(2) Kazemi, Z., Chang, H., Haserodt, S., McKen, C., and Zachara, N. E. (2010) O-linked beta-N-acetylglucosamine (O-GlcNAc) regulates stress-induced heat shock protein expression in a GSK-3beta-dependent manner. *J. Biol. Chem. 285*, 39096−39107.

(3) Zhu, Y., Shan, X., Yuzwa, S. A., and Vocadlo, D. J. (2014) The emerging link between O-GlcNAc and Alzheimer disease. *J. Biol. Chem. 289*, 34472−34481.

(4) Ferrer, C. M., Sodi, V. L., and Reginato, M. J. (2016) O-GlcNAcylation in Cancer Biology: Linking Metabolism and Signaling. *J. Mol. Biol. 428*, 3282−3294.

(5) Vocadlo, D. J. (2012) O-GlcNAc processing enzymes: catalytic mechanisms, substrate specificity, and enzyme regulation. *Curr. Opin. Chem. Biol. 16*, 488−497.

(6) Shen, D. L., Gloster, T. M., Yuzwa, S. A., and Vocadlo, D. J. (2012) Insights into O-linked N-acetylglucosamine ([0−9]O-GlcNAc) processing and dynamics through kinetic analysis of O-GlcNAc transferase and O-GlcNAcase activity on protein substrates. *J. Biol. Chem. 287*, 15395−15408.

(7) Yu, S. H., Boyce, M., Wands, A. M., Bond, M. R., Bertozzi, C. R., and Kohler, J. J. (2012) Metabolic labeling enables selective photocrosslinking of O-GlcNAc-modified proteins to their binding partners. *Proc. Natl. Acad. Sci. U. S. A. 109*, 4834−4839.

(8) Pathak, S., Alonso, J., Schimpl, M., Rafie, K., Blair, D. E., Borodkin, V. S., Schuttelkopf, A. W., Albarbarawi, O., and van Aalten, D. M. (2015) The active site of O-GlcNAc transferase imposes constraints on substrate sequence. *Nat. Struct. Mol. Biol. 22*, 744−750.

(9) Vocadlo, D. J., Hang, H. C., Kim, E. J., Hanover, J. A., and Bertozzi, C. R. (2003) A chemical approach for identifying *O*-GlcNAc-modified proteins in cells. *Proc. Natl. Acad. Sci. U. S. A. 100*, 9116−9121.

(10) Boyce, M., Carrico, I. S., Ganguli, A. S., Yu, S. H., Hangauer, M. J., Hubbard, S. C., Kohler, J. J., and Bertozzi, C. R. (2011) Metabolic cross-talk allows labeling of O-linked beta-N-acetylglucosamine-modified proteins via the N-acetylgalactosamine salvage pathway. *Proc. Natl. Acad. Sci. U. S. A. 108*, 3141−3146.

(11) Rexach, J. E., Rogers, C. J., Yu, S. H., Tao, J., Sun, Y. E., and Hsieh-Wilson, L. C. (2010) Quantification of O-glycosylation stoichiometry and dynamics using resolvable mass tags. *Nat. Chem. Biol. 6*, 645−651.

(12) Chuh, K. N., Zaro, B. W., Piller, F., Piller, V., and Pratt, M. R. (2014) Changes in metabolic chemical reporter structure yield a selective probe of O-GlcNAc modification. *J. Am. Chem. Soc. 136*, 12283−12295.

(13) Li, J., Wang, J., Wen, L., Zhu, H., Li, S., Huang, K., Jiang, K., Li, X., Ma, C., Qu, J., Parameswaran, A., Song, J., Zhao, W., and Wang, P. G. (2016) An OGA-resistant Probe Allow Specific Visualization and Accurate Identification of O-GlcNAc-modified Proteins in Cells. *ACS Chem. Biol. 11*, 3002.

(14) Lazarus, M. B., Nam, Y., Jiang, J., Sliz, P., and Walker, S. (2011) Structure of human O-GlcNAc transferase and its complex with a peptide substrate. *Nature 469*, 564−567.
(15) Lazarus, M. B., Jiang, J., Gloster, T. M., Zandberg, W. F., Whitworth, G. E., Vocadlo, D. J., and Walker, S. (2012) Structural snapshots of the reaction coordinate for O-GlcNAc transferase. *Nat. Chem. Biol. 8*, 966−968.
(16) Gloster, T. M., Zandberg, W. F., Heinonen, J. E., Shen, D. L., Deng, L., and Vocadlo, D. J. (2011) Hijacking a biosynthetic pathway yields a glycosyltransferase inhibitor within cells. *Nat. Chem. Biol. 7*, 174−181.
(17) Martinez-Fleites, C., Macauley, M. S., He, Y., Shen, D. L., Vocadlo, D. J., and Davies, G. J. (2008) Structure of an O-GlcNAc transferase homolog provides insight into intracellular glycosylation. *Nat. Struct. Mol. Biol. 15*, 764−765.
(18) Lubas, W. A., Smith, M., Starr, C. M., and Hanover, J. A. (1995) Analysis of nuclear pore protein p62 glycosylation. *Biochemistry 34*, 1686−1694.
(19) Zhu, Y., Liu, T. W., Madden, Z., Yuzwa, S. A., Murray, K., Cecioni, S., Zachara, N., and Vocadlo, D. J. (2016) Post-translational O-GlcNAcylation is essential for nuclear pore integrity and maintenance of the pore selectivity filter. *J. Mol. Cell Biol. 8*, 2−16.
(20) Hein, J. E., and Fokin, V. V. (2010) Copper-catalyzed azide-alkyne cycloaddition (CuAAC) and beyond: new reactivity of copper(I) acetylides. *Chem. Soc. Rev. 39*, 1302−1315.
(21) Meldal, M., and Tornoe, C. W. (2008) Cu-catalyzed azide-alkyne cycloaddition. *Chem. Rev. 108*, 2952−3015.
(22) Pathak, S., Borodkin, V. S., Albarbarawi, O., Campbell, D. G., Ibrahim, A., and van Aalten, D. M. (2012) O-GlcNAcylation of TAB1 modulates TAK1-mediated cytokine release. *EMBO J. 31*, 1394−1404.
(23) Lefebvre, T., Ferreira, S., Dupont-Wallois, L., Bussiere, T., Dupire, M. J., Delacourte, A., Michalski, J. C., and Caillet-Boudin, M. L. (2003) Evidence of a balance between phosphorylation and *O*-GlcNAc glycosylation of Tau proteins–a role in nuclear localization. *Biochim. Biophys. Acta, Gen. Subj. 1619*, 167−176.
(24) Dias, W. B., Cheung, W. D., Wang, Z., and Hart, G. W. (2009) Regulation of calcium/calmodulin-dependent kinase IV by O-GlcNAc modification. *J. Biol. Chem. 284*, 21327−21337.
(25) Zaro, B. W., Yang, Y. Y., Hang, H. C., and Pratt, M. R. (2011) Chemical reporters for fluorescent detection and identification of O-GlcNAc-modified proteins reveal glycosylation of the ubiquitin ligase NEDD4−1. *Proc. Natl. Acad. Sci. U. S. A. 108*, 8146−8151.
(26) Piller, F., Hanlon, M. H., and Hill, R. L. (1983) Co-purification and characterization of UDP-glucose 4-epimerase and UDP-N-acetylglucosamine 4-epimerase from porcine submaxillary glands. *J. Biol. Chem. 258*, 10774−10778.
(27) Datema, R., and Schwarz, R. T. (1978) Formation of 2-deoxyglucose-containing lipid-linked oligosaccharides. Interference with glycosylation of glycoproteins. *Eur. J. Biochem. 90*, 505−516.
(28) Holt, G. D., Snow, C. M., Senior, A., Haltiwanger, R. S., Gerace, L., and Hart, G. W. (1987) Nuclear pore complex glycoproteins contain cytoplasmically disposed O-linked N-acetylglucosamine. *J. Cell Biol. 104*, 1157−1164.
(29) Cieniewski-Bernard, C., Bastide, B., Lefebvre, T., Lemoine, J., Mounier, Y., and Michalski, J. C. (2004) Identification of O-linked N-acetylglucosamine proteins in rat skeletal muscle using two-dimensional gel electrophoresis and mass spectrometry. *Mol. Cell. Proteomics 3*, 577−585.
(30) Wells, L., Vosseller, K., Cole, R. N., Cronshaw, J. M., Matunis, M. J., and Hart, G. W. (2002) Mapping sites of O-GlcNAc modification using affinity tags for serine and threonine post-translational modifications. *Mol. Cell. Proteomics 1*, 791−804.
(31) Wang, Z., Pandey, A., and Hart, G. W. (2007) Dynamic interplay between O-linked N-acetylglucosaminylation and glycogen synthase kinase-3-dependent phosphorylation. *Mol. Cell. Proteomics 6*, 1365−1379.
(32) Palaniappan, K. K., Hangauer, M. J., Smith, T. J., Smart, B. P., Pitcher, A. A., Cheng, E. H., Bertozzi, C. R., and Boyce, M. (2013) A chemical glycoproteomics platform reveals O-GlcNAcylation of mitochondrial voltage-dependent anion channel 2. *Cell Rep. 5*, 546−552.
(33) Nangle, L. A., Motta, C. M., and Schimmel, P. (2006) Global effects of mistranslation from an editing defect in mammalian cells. *Chem. Biol. 13*, 1091−1100.
(34) Hellerstein, M. K., Letscher, A., Schwarz, J. M., Cesar, D., Shackleton, C. H., Turner, S., Neese, R., Wu, K., Bock, S., and Kaempfer, S. (1997) Measurement of hepatic Ra UDP-glucose in vivo in rats: relation to glycogen deposition and labeling patterns. *Am. J. Physiol. 272*, E155−162.
(35) Hawkins, M., Angelov, I., Liu, R., Barzilai, N., and Rossetti, L. (1997) The tissue concentration of UDP-N-acetylglucosamine modulates the stimulatory effect of insulin on skeletal muscle glucose uptake. *J. Biol. Chem. 272*, 4889−4895.
(36) Macauley, M. S., Whitworth, G. E., Debowski, A. W., Chin, D., and Vocadlo, D. J. (2005) O-GlcNAcase uses substrate-assisted catalysis: kinetic analysis and development of highly selective mechanism-inspired inhibitors. *J. Biol. Chem. 280*, 25313−25322.
(37) Sols, A., and Crane, R. K. (1954) Substrate specificity of brain hexokinase. *J. Biol. Chem. 210*, 581−595.
(38) Sinclair, D. A., Syrzycka, M., Macauley, M. S., Rastgardani, T., Komljenovic, I., Vocadlo, D. J., Brock, H. W., and Honda, B. M. (2009) Drosophila O-GlcNAc transferase (OGT) is encoded by the Polycomb group (PcG) gene, super sex combs (sxc). *Proc. Natl. Acad. Sci. U. S. A. 106*, 13427−13432.
(39) Gambetta, M. C., Oktaba, K., and Muller, J. (2009) Essential role of the glycosyltransferase sxc/Ogt in polycomb repression. *Science 325*, 93−96.
(40) Liu, T. W., Myschyshyn, M., Sinclair, D., Cecioni, S., Beja, K., Honda, B., Morin, R., and Vocadlo, D. J. (2016) Genome-wide chemical mapping of O-GlcNAcylated proteins in Drosophila melanogaster. *Nat. Chem. Biol.*, DOI: 10.1038/nchembio.2247.
(41) Schulz, T. J., Zarse, K., Voigt, A., Urban, N., Birringer, M., and Ristow, M. (2007) Glucose restriction extends Caenorhabditis elegans life span by inducing mitochondrial respiration and increasing oxidative stress. *Cell Metab. 6*, 280−293.
(42) Ralser, M., Wamelink, M. M., Struys, E. A., Joppich, C., Krobitsch, S., Jakobs, C., and Lehrach, H. (2008) A catabolic block does not sufficiently explain how 2-deoxy-D-glucose inhibits cell growth. *Proc. Natl. Acad. Sci. U. S. A. 105*, 17807−17811.
(43) Kang, H. T., Ju, J. W., Cho, J. W., and Hwang, E. S. (2003) Down-regulation of Sp1 activity through modulation of O-glycosylation by treatment with a low glucose mimetic, 2-deoxyglucose. *J. Biol. Chem. 278*, 51223−51231.
(44) Hellerstein, M. K., Neese, R. A., Schwarz, J. M., Turner, S., Faix, D., and Wu, K. (1997) Altered fluxes responsible for reduced hepatic glucose production and gluconeogenesis by exogenous glucose in rats. *Am. J. Physiol. 272*, E163−172.
(45) Hellerstein, M. K., Kaempfer, S., Reid, J. S., Wu, K., and Shackleton, C. H. (1995) Rate of glucose entry into hepatic uridine diphosphoglucose by the direct pathway in fasted and fed states in normal humans. *Metab., Clin. Exp. 44*, 172−182.
(46) Haltiwanger, R. S., Blomberg, M. A., and Hart, G. W. (1992) Glycosylation of nuclear and cytoplasmic proteins. Purification and characterization of a uridine diphospho-N-acetylglucosamine:polypeptide beta-N-acetylglucosaminyltransferase. *J. Biol. Chem. 267*, 9005−9013.
(47) Leatherbarrow, R. J. (2001) *GraFit Version 5*, Erithacus Software Ltd., Horley, UK.